

Measurements of the electron-phonon interaction in Nb by inelastic neutron scattering*

S. M. Shapiro, G. Shirane, and J. D. Axe

Brookhaven National Laboratory, Upton, New York 11973

(Received 1 April 1975)

Precise linewidth and frequency measurements of transverse acoustic modes propagating along the [001] and [110] directions were performed on single crystals of niobium in the normal and superconducting phases ($T_c = 9.2^\circ\text{K}$). For transverse phonons propagating along the [110] direction changes in linewidth are observed when the superconducting gap $2\Delta(T)$ equals the phonon frequency. This behavior agrees with Bobetic's calculation for the attenuation of high-frequency sound waves in superconductors and the magnitude of the change enables us to calculate the electron-phonon interactions. In addition to linewidth changes, anomalous temperature dependence of the peak position of some acoustic modes is also observed. The [001] transverse phonons exhibit a decrease of $\sim 15\%$ when T is decreased from 300°K to T_c . Below T_c there is an additional softening of 3% . This softening extends along the $[\xi 00]$ direction to $\xi = 0.5$, the limit of our measurements.

I. INTRODUCTION

The electron-phonon (e - p) interactions play a fundamental role in the occurrence of superconductivity.¹ The interaction between the electrons which leads to the formation of Cooper pairs is mediated by the ever-present phonon fields. Knowledge about the e - p interactions in metals can lead to a more complete understanding of superconductivity and ultimately guide us in the selection of materials to combine to form high- T_c superconductors.

Within the BCS theory of superconductivity² the e - p interactions have been parametrized in several ways. The electron-phonon spectral function $\alpha^2(\omega)F(\omega)$ is the square of an average electron-phonon interaction, $\alpha^2(\omega)$, times the phonon density of states, $F(\omega)$. This product is related to the dimensionless electron-phonon coupling parameter, λ ,³

$$\lambda \equiv 2 \int_0^{\omega_0} \frac{\alpha^2(\omega)F(\omega)}{\omega} d\omega, \quad (1)$$

where the integration is over the phonon frequencies. λ corresponds roughly to the product $N_i(0)V$ of BCS, where $N_i(0)$ is the electronic density of states at the Fermi surface for a single spin orientation and V is the pairing potential arising from the e - p interaction. McMillan³ has derived a relationship between λ and T_c which enables one, in principle, to calculate T_c from the material properties of the normal state.

Measurements of the e - p interaction in superconductors have been limited mainly to tunneling experiments,⁴ where, in favorable cases, $\alpha^2(\omega) \times F(\omega)$ can be deduced. If $F(\omega)$ is known from other measurements, $\alpha^2(\omega)$ can be obtained. Unfortunately, in addition to this being an indirect method of measuring the e - p interaction, the results are often dependent on junction preparations.

Recently Allen⁵ has shown that the parameter λ

is related to the linewidth of the phonon resonance in the dynamical structure factor $S(q, \omega)$, as measured by scattering experiments. The additional linewidth $2\Gamma_q^{e-p}$ given to the phonons due to coupling to the electrons is basically the imaginary part of the phonon self-energy due to the e - p interaction and is given by

$$2\Gamma_q^{e-p} = 2\pi N_i(0) \hbar\omega_q^2 \lambda_q, \quad (2)$$

where λ_q is the contribution to λ from the phonon q , i. e., $\lambda = (1/3N) \sum_q \lambda_q$ and N is the number of atoms in the crystal. With the above relationship, a measurement of a phonon linewidth plus knowledge of other properties such as the density of electron states can yield a measurement of the electron-phonon coupling parameter λ .

At a given frequency $2\Gamma_q^{e-p}$ is proportional to the sound-attenuation constant α .⁶ The BCS theory describes α in the superconducting (S) and normal (N) states. The ratio of the sound attenuation in the S and N states is¹

$$\frac{\alpha_S}{\alpha_N} = \frac{1}{\hbar\omega_p} \int \left(1 - \frac{\Delta^2}{EE'}\right) [f(E) - f(E')] \times N_i(E)N_i(E') dE, \quad (3)$$

where the integral is over the electron energies measured relative to the Fermi energy. The Fermi factor $f(E)$ is

$$f(E) = (e^{E/kT} + 1)^{-1}$$

and $E' = E + \hbar\omega_p$ with $\hbar\omega_p$ the phonon energy. $N_i(E)$ is the density of electronic states in energy with

$$N_i(E) = 0, \quad |E| < \Delta(T)$$

$$N_i(E) = E/(E^2 - \Delta^2)^{1/2}, \quad |E| > \Delta(T)$$

with $2\Delta(T)$ being the temperature-dependent superconducting gap. In most ultrasonic experiments the phonon frequencies are much less than the gap energy [$\hbar\omega_p \ll \Delta(0)$] and we set $E = E'$ within the in-

tegral except for the exponential. Integration yields

$$\alpha_S/\alpha_N = f(\Delta)/f(0) = 2f(\Delta). \quad (4)$$

This simple relation results from the fact that in the ultrasonic frequency regime the sound wave interacts only with quasiparticles that are thermally excited above the $2\Delta(T)$ gap. Below T_c the low-frequency sound wave has insufficient energy to break up the Cooper pairs and the attenuation depends only upon the number of particles thermally excited above the Fermi energy which is given by $f(\Delta)$. The relation has been shown to fit observed attenuation data in several metals with simple Fermi surfaces⁷ and has been a useful method of measuring $\Delta(T)$ and its anisotropy even in more complicated metals. So far as we are aware only measurements of the ratio α_S/α_N have been made ultrasonically, which does not determine the electron-phonon coupling strength.

Privorotskii,⁸ Bobetic,⁹ and others¹⁰ evaluated Eq. (3) for phonon frequencies approaching $2\Delta(T)$. In this frequency regime the results are not as simple as Eq. (4) since the phonon now is energetically able to break up the Cooper pairs and an additional damping mechanism is available. One expects sharp discontinuities of the attenuation superimposed upon the $f(\Delta)$ behavior as the resonant condition $\hbar\omega_p = 2\Delta(T)$ is approached.

Although the theoretical results^{8,9} for arbitrary $\hbar\omega_p$ and temperature T cannot be obtained in closed form, one can calculate the jump δ in the ratio α_S/α_N at $\hbar\omega = 2\Delta(T)$:

$$\delta(\alpha_S/\alpha_N) = \frac{1}{2}\pi[1 - 2f(\Delta)]. \quad (5)$$

The jump is very small at temperatures near T_c and has a maximum value of 1.57 at $T=0$. Thus we expect to have an attenuation exceeding that of the normal state when the pair-breaking energy condition $\hbar\omega_p = 2\Delta(T)$ is satisfied. This is due to the large density of electronic states at the gap energy resulting in more quasiparticles to interact with than on either side of the 2Δ gap. This similar enhancement, $\alpha_S/\alpha_N > 1$, persists for $\hbar\omega_p > 2\Delta(0)$. Here the phonon always has sufficient energy to break up the Cooper pairs. For fixed frequencies only slightly larger than $2\Delta(0)$, the singularity in the electronic density of states at $\hbar\omega_p = 2\Delta(T)$ will be approached as T is decreased and correspondingly, the attenuation will increase. The increase in phonon linewidth is directly related to the pair-breaking processes and can be used to obtain a measure of the λ_q parameter via Eq. (2). One has a more direct method than tunneling for measuring the e - p interactions.

For high- T_c superconductors, $2\Delta(0)$ is much larger than obtainable ultrasonic frequencies and pair-breaking contribution to the above theory has

been difficult to confirm. Only in materials where $T_c \sim 1^\circ\text{K}$ or less can ultrasonic methods probe the pair-breaking mechanism of the phonon, and in these experiments the complete predictions of the theory have not been confirmed.¹¹

Inelastic neutron scattering has been shown to be a useful tool for measuring the phonon linewidth at frequencies near the gap energy.¹² The "tuning" of the frequency is achieved by varying the wave vector $\vec{\zeta} \equiv \vec{q}a/2\pi$ of the phonon. By studying several directions of propagation, the anisotropy of the linewidth and λ can also be measured.

The first experiment of this sort was performed on Nb_3Sn , a strong-coupling high- T_c material.¹² The increase in linewidth near T_c is large but the single crystals were extremely small ($\sim 0.05\text{ cm}^3$) and prevented any precise verification of the theory. In an earlier paper, we measured the phonon linewidth on large single crystals of niobium and showed these results to be in qualitative agreement with BCS theory.¹³ Below, we describe in more detail an estimate of $2\Gamma_q^{e-p}$ which can be compared to that calculated by Allen. In addition the effects of a magnetic field and the frequency dependence of the linewidth are explored.

In measuring the phonon linewidth we are probing the imaginary part of the phonon self-energy. A natural question to pose is: "What happens to the real part of this self-energy when a metal becomes superconducting?" Ultrasonic studies¹⁴ have shown for Nb, Pb, and V that the elastic constants *decrease* by $\leq 0.01\%$ when the sample is cooled to the superconducting state, in contradiction to what is expected from anharmonic lattice contributions.¹⁵ The reason for this is not as physically apparent as in the linewidth case, but there have been some recent calculations¹⁶ showing the behavior of the phonon frequencies near the superconducting transition. We shall show below that for some transverse modes propagating along the [001] direction, there is a large decrease ($\sim 15\%$) in the frequency of the phonons as the crystal is cooled down from $T=300$ to 1.6°K .

II. EXPERIMENTAL

The inelastic neutron scattering measurements were performed on a triple-axis spectrometer at the Brookhaven High Flux Beam Reactor. Pyrolytic graphite crystals were used as the monochromator, analyzer, and filter. Two single crystals of Nb were obtained commercially¹⁷ and specially selected for their narrow mosaic. They were cylindrical in shape with a diameter of 1 cm and a length of 3 cm. The sample mosaic spreads measured with a perfect analyzer were 5 and 12 min. The narrower mosaic crystal has its cylindrical axis along the [110] direction and was used for the linewidth measurements. The other crystal has

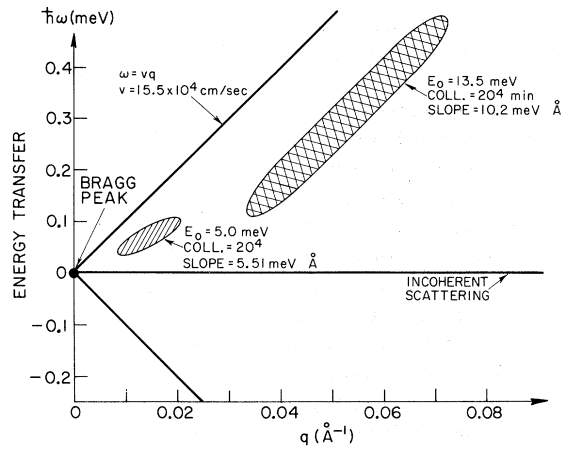


FIG. 1. Triple-axis spectrometer resolution function calculated (Ref. 18) for 13.5- and 5.0-meV incident-neutron energy demonstrating the effect of focusing.

the cylindrical axis along the [001] direction and was used for most of the frequency-shift measurements.

The typical value of 2Γ in Nb has been estimated to be $\frac{1}{4}$ of that for Nb_3Sn .⁵ Thus, in comparison with Ref. 12, an observed linewidth considerably smaller than in Nb_3Sn was expected. It would have been impossible to observe the linewidth had it not been for the availability of excellent quality single crystals of Nb and the "focusing" of the neutron spectrometer's resolution function. This focusing effect is shown in Fig. 1. The cross-hatched ellipses are the ω - q projection of the triple-axis spectrometer's resolution function for a transverse scan.¹⁸ The sloping lines represent the phonon dispersion curve for acoustic modes with a velocity of 15.5×10^4 cm/sec nearly the same as that of the resolution ellipse for incident-neutron energy of 13.5 meV monochromatized and analyzed by pyrolytic graphite crystals with 20-min horizontal collimation throughout the instrument. A constant- \bar{Q} energy scan essentially moves the resolution function through the dispersion curve. For this "perfect focusing" condition (sound velocity equals neutron velocity) and assuming no intrinsic phonon width, it is easily seen that the energy linewidth of the observed peak will be the energy width of the center of the resolution function. If the phonon now has an intrinsic width, the observed linewidth will be the convolution of the known instrumental resolution with the phonon response function. If the intrinsic width is large enough, one should be able to detect it and properly subtract the resolution part of the observed width.

If one relaxes the focusing condition and makes the resolution slope less than the sound velocity by changing the incident energy a linewidth broader

than the central part of the resolution function would be observed. The smaller hatched area shows the resolution function for 5.0-meV incident-neutron energy. For a constant- \bar{Q} scan with this incident energy, the observed width corresponds almost to the total height of the resolution function, which is nearly the same as the central part of the 13.5-meV resolution function. Thus one gains only in momentum resolution by using the lower incident energy and one loses considerable intensity owing to the decreased size of the resolution function and the lower reactor flux at 5.0 meV.

III. RESULTS

A. Linewidth measurements

The bulk of the linewidth measurements were made on the $[110]T_2$ branch of the narrow mosaic crystal since it is for this branch that the focusing occurs. Figure 2 shows the spectra of the $[110]T_2$ mode obtained at $T = 7.5^\circ\text{K}$, where $\hbar\omega_p = 2\Delta(T)$, and at $T = 2.5^\circ\text{K}$, where $\hbar\omega_p < 2\Delta(T)$. That a broadening occurs is most obvious from the increase in the peak intensity as T is lowered. Since the integrated intensity is proportional to the occupation factor $1 + n(\omega)$, with $n(\omega) = (e^{\hbar\omega/kT} - 1)^{-1}$, a decrease in T causes a decrease in total intensity. The increase in the peak intensity for lower

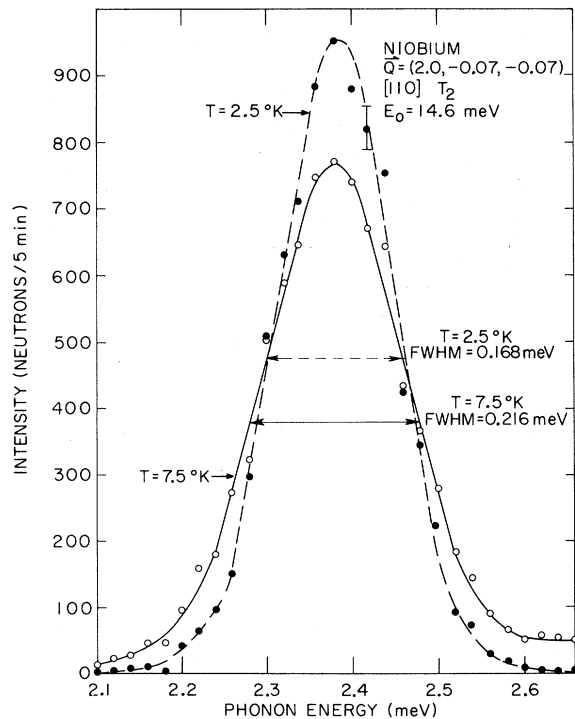


FIG. 2. Neutron group of $[\xi\xi\xi]T_2$, $\xi = 0.07$ phonon showing change in FWHM as the sample becomes superconducting. This corresponds to curve A of Fig. 3.

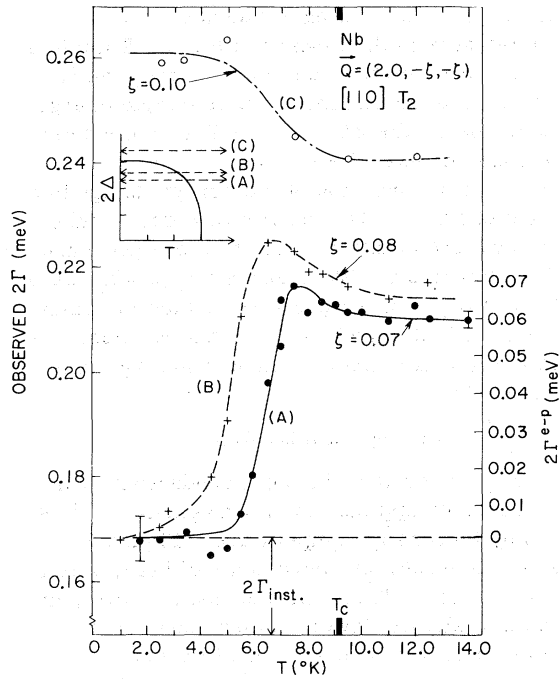


FIG. 3. Temperature dependence of several $[\xi\xi 0]T_2$ phonons in Nb showing the change in width due to the superconducting gap. Curves A and B have $\hbar\omega_p < 2\Delta(0)$ and for curve C, $\hbar\omega_p > 2\Delta(0)$.

T logically implies a narrower linewidth.

A measure of the peak positions and linewidths was determined by calculating the first and second moments of the intensity distribution. The relative statistical accuracy is of order $1/\sqrt{N}$, where N is the total number of counts in one peak: ~ 5000 counts. This method of determining the position and width is a sensitive way of measuring changes as a function of temperature (or field) where the scans are always over the same region. By multiplying the linewidth obtained from the moment technique by $2\sqrt{2\ln 2}$, which converts the $1/e$ width to a full width at half-maximum (FWHM) of

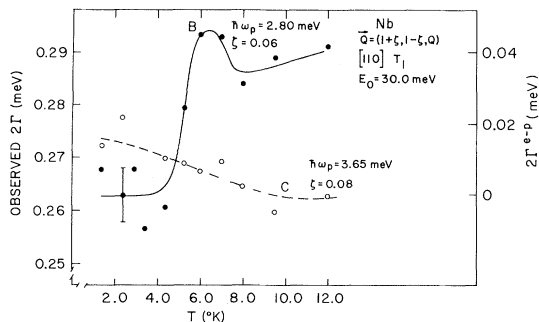


FIG. 4. Temperature dependence of the linewidth of two phonons on the $[\xi\xi 0]T_1$ branch in Nb. For $\zeta = 0.06$, $\hbar\omega_p < 2\Delta(0)$ and $\zeta = 0.08$, $\hbar\omega_p > 2\Delta(0)$.

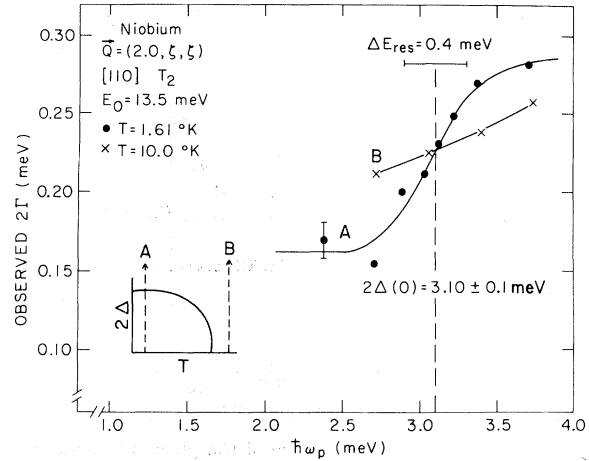


FIG. 5. Frequency dependence of the phonon linewidth on the $[110]T_2$ branch. Curve A is with $T < T_c$ and curve B with $T > T_c$.

a Gaussian distribution, we obtain good agreement with the observed width.

Figure 3 shows the observed linewidth 2Γ vs temperature for several $[110]T_2$ phonons. Curves A and B are for phonon energies less than $2\Delta(0)$ and the resonance condition $\hbar\omega_p = 2\Delta(T)$ is achieved for $T < T_c$. Curve C has a phonon energy greater than 2Δ for all temperatures. The linewidth at the lowest temperature for A is assumed to be that of the instrumental resolution, implying that at these low temperatures, any phonon-phonon interaction is small. It was approximately verified by comparing the linewidth generated by a modified version of a computer calculation¹⁹ which analytically performs energy scans through an infinitely sharp dispersion surface using the full four dimensions of the resolution function. The measured linewidth was 20% narrower than the calculated value and is presumed to be due to improper consideration of the vertical collimation.

We use this low-temperature Gaussian width as the instrumental resolution. Since the intrinsic line shape of the phonon is most likely Lorentzian, the contribution to the observed linewidth from the e - p interaction can be extracted by numerical techniques.²⁰ The right-hand sides of Figs. 3 and 4 show the intrinsic e - p interaction. At the resonant condition $\hbar\omega_p = 2\Delta(T)$, the electron-phonon contribution to the linewidth is $2\Gamma^{e-p} = 0.06 \pm 0.01$ meV for $\zeta = 0.07$. For temperatures $T > T_c$, in the normal state, the linewidths of the three phonons measured are different owing either to an increase in phonon-phonon interactions or a q dependence of the electron-phonon interaction. Because of the uncertainty of this contribution it is not possible to properly normalize the three curves. Quantitative values are valid only for $\zeta = 0.07$.

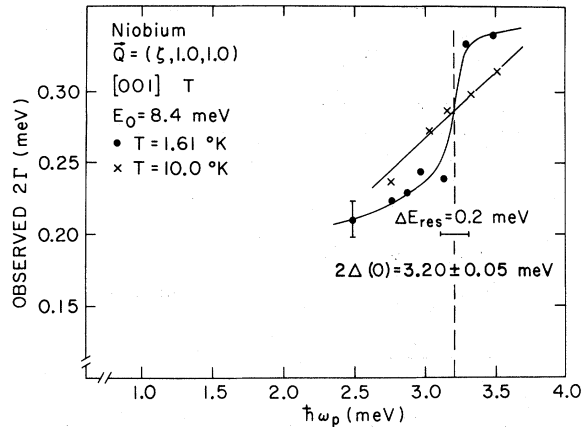


FIG. 6. Frequency dependence of the phonon linewidth on the [001]T branch.

We also measured the temperature-dependent linewidth of the T_1 mode propagating along the [110] direction with polarization along [110]. This mode has a higher velocity than T_2 . The experiments were performed with 30.0-meV incident-neutron energy, with pyrolytic graphite [004] for monochromator and analyzer in order to approach the focusing condition and still have a relatively good resolution. The results are shown in Fig. 4 for two phonons: $\zeta = 0.06$ with $\hbar\omega_p < 2\Delta(0)$, and $\zeta = 0.08$ with $\hbar\omega_p > 2\Delta(0)$. The results are similar to that observed in Fig. 3 for curves A and C. Because of the higher resolution the observed intensity was less and the accuracy of the measurements is reduced. Nevertheless the change in linewidth due to the onset of superconductivity is apparent.

The e - p contribution of the phonon linewidth can also be studied by keeping the sample at a constant temperature and varying the phonon frequency (see insert in Fig. 5). An additional contribution to the linewidth is again expected at the resonance condition $\hbar\omega_p = 2\Delta(T)$ of the size given in Eq. (5).⁹ If these measurements are performed at sufficiently low temperatures the technique is ideal for measuring the superconducting gap $2\Delta(0)$ and its anisotropy. Figures 5 and 6 show the results for transverse phonons propagating along [110] and [001] directions, respectively. Curve A is a scan made at low temperature where the resonant condition $\hbar\omega_p = 2\Delta(T)$ can be achieved. Curve B corresponds to scans in the normal state. The increase in linewidth for increasing frequency in the normal state may be due to an increase in phonon-phonon interaction or a q dependence of the e - p interaction. Curve A shows an abrupt increase in the linewidth as the 2Δ curve is crossed. In these measurements, the important factor in determining the abruptness of the change is not the focusing condition, but the total energy height of the resolution

function. This is most easily seen if we consider the energy axis in the insert of Fig. 5. If the total height of the resolution function is large, the finite size of the resolution function will sample energies above and below the 2Δ curves. This contributes to the rounding near the 2Δ value.

The frequency position of the abrupt change is a measure of $2\Delta(T)$. The results in Figs. 5 and 6 give a measure of $2\Delta(T = 1.61 \text{ °K})$ along [110] and [001], respectively. We observe $2\Delta_{[110]} = 3.1 \pm 0.1$ meV and $2\Delta_{[001]} = 3.20 \pm 0.5$ meV, which is consistent with a slight anisotropy and in agreement with ultrasonic results⁷ and the latest tunneling measurements.²¹

B. Magnetic field effects

It is well known that the superconductivity can be destroyed by application of a magnetic field as well as by increasing temperature. Figure 7 shows the linewidth measurements of [110] T_2 as a function of field. These measurements were performed at a slightly lower incident-neutron energy, with a slight defocusing condition which accounts for the broader linewidths at zero field. In this experiment the sample temperature was 4.4 °K and the magnetic field was varied. The same three phonons were measured as in Fig. 3 and we

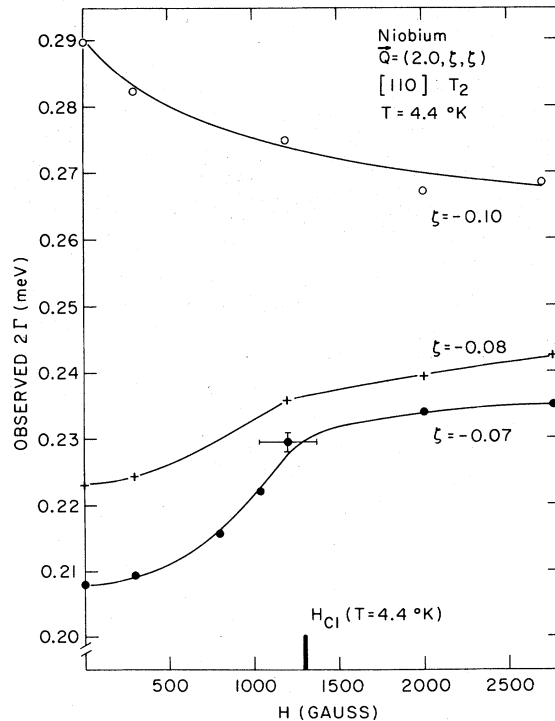


FIG. 7. Magnetic field dependence of the linewidth of several $[\xi \zeta 0]T_2$ phonons in Nb. For $\zeta = 0.07$ and 0.08 , $\hbar\omega_p < 2\Delta(0)$ and for $\zeta = 0.10$, $\hbar\omega_p > 2\Delta(0)$. H_{c1} is taken from Ref. 22.

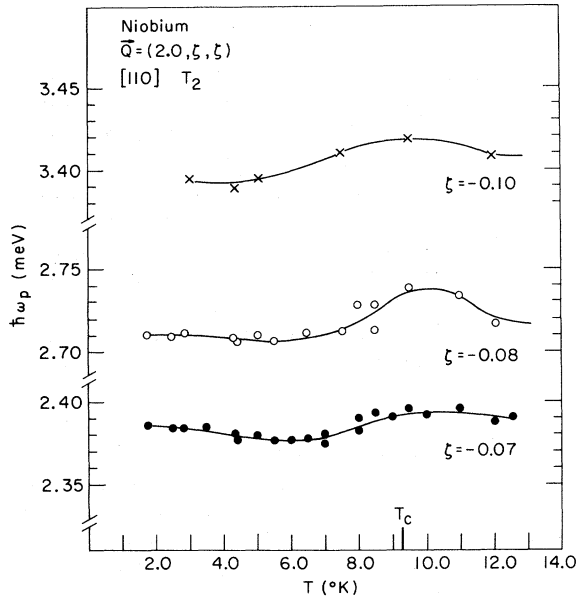


FIG. 8. Temperature dependence of the energy of several $[110]T_2$ phonons at low temperatures.

see the same qualitative behavior, only the abscissa is now the magnetic field: an increase in linewidth up to H_{C1} for phonon energy $\hbar\omega_p < 2\Delta(H=0)$ and a decrease in linewidth with increasing field for phonon energy $\hbar\omega_p > 2\Delta(H=0)$. The field where the linewidth changes corresponds to the critical field $H_{C1} = 1300 \pm 100$ G for Nb.²² These results are qualitatively understood if there exists below H_{C1} an intermediate state where, because of geometrical effects, the field can penetrate the sample and normal regions develop in the superconductor.²³ As H increases, the normal regions become larger and there are, averaged over the crystal size, more "broken" Cooper pairs for the phonons to interact with.

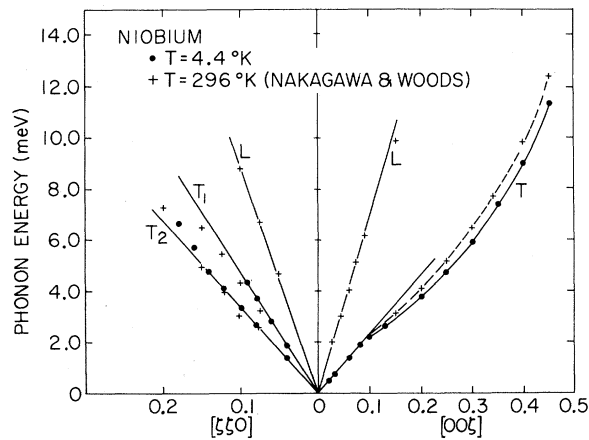


FIG. 9. Low- q behavior of phonon dispersion curve along $[001]$ and $[110]$ directions for Nb. Room-temperature data is from Ref. 24.

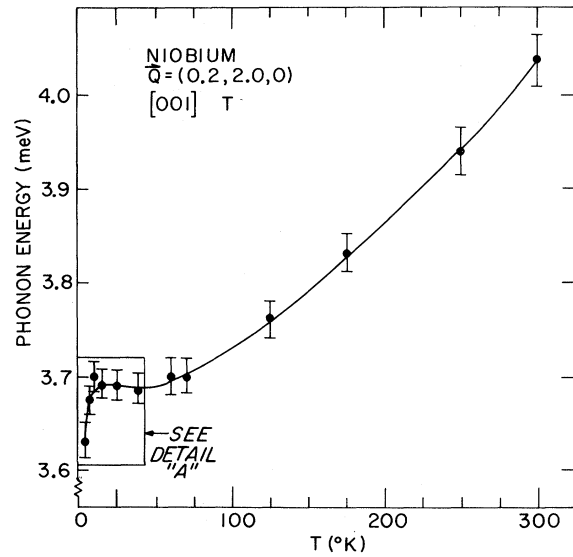
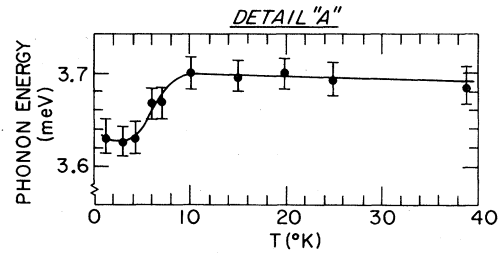


FIG. 10. Temperature dependence of the $[00\xi]T$, $\zeta = 0.2$ phonon showing the anomalous softening for $T_c < T < 300^\circ\text{K}$ and an additional softening for $T < T_c$.



C. Line-shift measurements

After having studied the temperature dependence of the energy linewidth of the $[110]T_2$ branch we now examine what happens to the real part of the self-energy of the phonons as Nb becomes superconducting. Figure 8 shows the behavior of the peak positions of the three phonons studied above. They show essentially the same behavior: an increase of phonon energy near T_c and then a subsequent decrease for T less than T_c . The changes are quite small, $\sim 1\%$, but are larger than the accuracy of the measurements and are reproducible.

A more dramatic effect is observed in the $[00\xi]T$ branch. Figure 9 shows the low- q region of the phonon dispersion curves in the $[001]$ and $[110]$ directions. Room-temperature data are from Ref. 24 and our results for 4.2°K are given. There is an unusual curvature of the $[00\xi]T$ (Δ_5) branch from $\zeta \geq 0.1$ which persists up to 1056°K ,²⁵ but decreases with Mo alloying.²⁶ The temperature dependence of this branch is anomalous; for $\zeta > 0.1$, the frequency decreases with decreasing temperature, contrary to the expected behavior. Figure 10 shows the behavior of the phonon energy for $\zeta = 0.2$ from 300

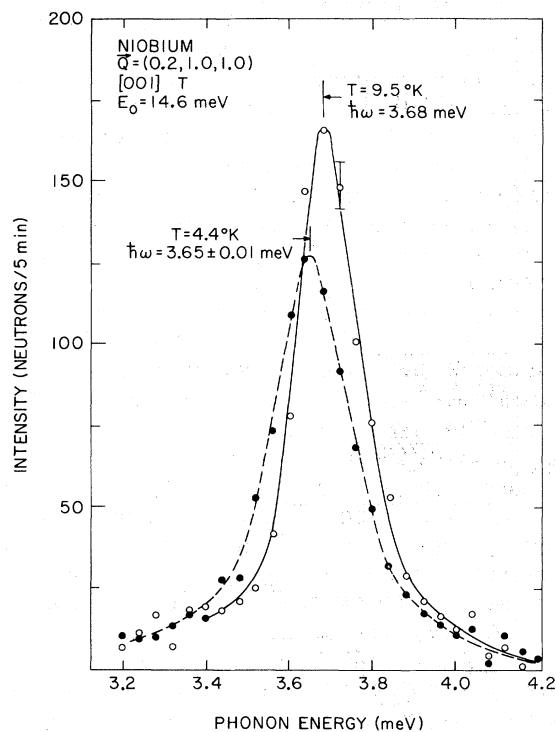


FIG. 11. Scattered-neutron spectra of the $[00\xi]T$, $\xi=0.2$ phonon for $T > T_c$ (solid line) and $T < T_c$ (dashed line) showing decrease in energy with decrease in temperature.

down to 1.6 °K. Between 300 and 10 °K there is ~15% decrease in frequency. An additional, unexpected 3% softening is seen as Nb becomes superconducting for $T < 9.2$ °K. Figure 11 shows the spectra above and below T_c . The shift, though small, is quite evident and this figure reveals the sensitivity of our measurements to changes in peak position of the spectra. The insert in Fig. 10 shows the temperature-dependent behavior of this phonon within the superconducting region. This low-temperature behavior was studied for phonon momentum up to $\xi=0.50$ along the $[001]$ direction.

Because of this anomalous behavior in the dispersion curve it was impossible to obtain reliable measurements of the linewidth along this branch. Since the dispersion changes as a function of temperature the contribution due to intrinsic broadening of the phonon and broadening due to the change in curvature within the resolution function are difficult to separate.

It was not possible to measure any broadening of longitudinal modes because of the much larger instrumental resolution for longitudinal scans.¹⁸ However, the dip in the $[001]L$ branch²⁴ was studied at 4.35 °K and also showed a 3% softening compared to room temperature.

IV. DISCUSSION

The linewidth measurements shown in Fig. 3 confirm the results of Bobetic's calculations for high-frequency sound. In Fig. 12, we show the theoretical behavior of the attenuation of sound at the frequency corresponding to curve A in Fig. 3 and compare it with the data. The infinite slope at $\hbar\omega_p = 2\Delta(T)$ is due to the square-root singularity of the density of states. The smoothing of the discontinuities in the observed data is partly due to the finite height of the resolution function, since for temperatures near where $\hbar\omega_p = 2\Delta(T)$, part of the resolution function samples energies greater and less than 2Δ . The temperature region where this is calculated to be important is indicated in the figure. This accounts for some of the smoothing of the discontinuity but not all. The additional contribution may be a measure of the gap anisotropy since Γ_q^{e-p} at these small q 's samples a belt around the Fermi surface.

The theory also predicts the magnitude of the jump in the absorption at $\hbar\omega_p = 2\Delta(T)$ [Eq. (5)]. For the frequency of Fig. 12, the calculated jump is

$$\delta(\alpha_S/\alpha_N)_{\text{calc}} = 1.2 \text{ at } 2\Delta = 2.4 \text{ meV.}$$

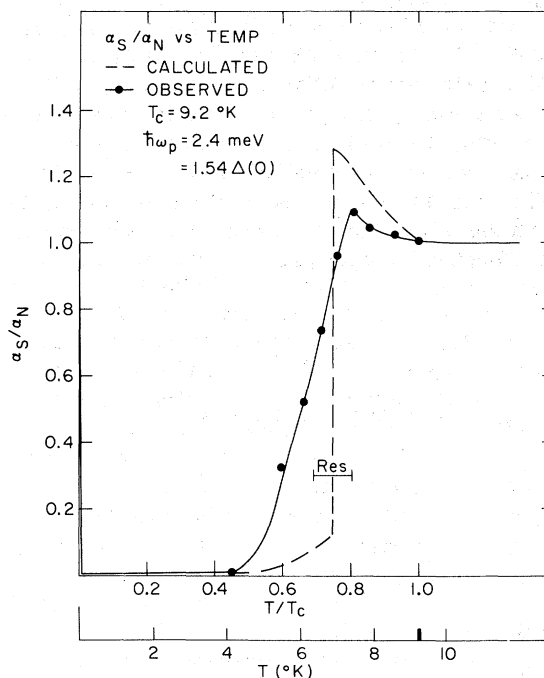


FIG. 12. Temperature dependence of the ratio of the attenuation of sound in the superconducting state (α_S) to the sound attenuation in the normal state (α_N) for phonon energy $\hbar\omega_p = 2.37$ meV: $\hbar\omega_p/2\Delta(0) = 0.76$. Dashed line is from Bobetic's (Ref. 9) calculation. Solid line is the temperature dependence of the phonon linewidth (curve A in Fig. 3).

The observed value is

$$\delta(\alpha_S/\alpha_N)_{\text{obs}} = 1.1 \pm 0.1,$$

in good agreement with theory. An initially surprising result of the theory, confirmed in the experiment, is that for $\hbar\omega_p = 2\Delta(T)$, the attenuation of sound exceeds that in the normal state. This more subtle feature of high-frequency attenuation was not observable in the earlier experiments^{11,12} and provides a convincing confirmation of the theory.

There still remain a few comments to be made, however. The theory⁸⁻¹⁰ considers attenuation of longitudinal sound waves and implies a simple spherical Fermi surface. Our results show that the effect also exists for transverse modes and a system where the Fermi surface is not simple. For transverse modes one has to also consider the electromagnetic effects of attenuation due to eddy-current damping of the magnetic fields set up by the transverse phonons. In the superconducting state this field is reduced by the Meissner effect and a discontinuous drop of the transverse-acoustic attenuation is expected upon entering into the superconducting state.²⁷ Because of the enhancement of the attenuation observed just upon entering the superconducting state, we conclude that the pair-breaking mechanism dominates the attenuation.

We can compare our measurements with the theory presented by Allen.⁵ Using the data for $[\xi\xi 0]T_2$, $\zeta = 0.07$ we obtain

$$2\Gamma_q^{e-p}/\omega_q = 0.03 \pm 0.01.$$

If one uses the average quantities in Eq. (2) and the appropriate values in the literature,²⁸ we obtain $\langle 2\Gamma_q^{e-p}/\omega_q \rangle_{\text{av}} = 0.025$, which is in agreement with the observation.

Allen recently tried to estimate the importance of a phonon for T_c by considering the reduction in T_c if the electron-phonon interaction of the particular phonon is turned off.²⁹ He found that the low frequency phonon studied above has $3\frac{1}{2}$ times as much influence on T_c as the average phonon, a result consistent with the larger $e-p$ interaction. Allen further emphasized that the occurrence of superconductivity in Nb_3Sn represents a more extreme case of the anomalous behavior seen in Nb. A more complete understanding of the latter may yield the required knowledge to explain the high T_c of the former.

Selection rules for acoustic-phonon damping in cubic metals have been calculated for a near-neighbor tight-binding metal.³⁰ For a bcc metal such as Nb, no contribution to the linewidth from the electron-phonon interaction for the $[110]T_1$ phonon is expected. It is clear in Fig. 4 that we are seeing an interaction of about the same strength as for the $[110]T_2$ phonon.

A complete understanding of the temperature-dependent behavior of the phonon energy as shown in Fig. 10 is lacking. It appears the behavior can be divided into two temperature regimes: $T < T_c$ and $T > T_c$. For $T < T_c$ the data are summarized in Fig. 13, where we plot the percentage change of the frequency along the $[001]T$ branch where the normal frequency is taken as the value at 10 °K. For phonon frequencies less than 1.5 meV there is no change as a function of temperature. As the frequency increases the softening increases and there seems to be a minimum near $\hbar\omega_N \sim 3.0$ meV which closely corresponds to the $2\Delta(0)$ value. Schuster¹⁶ has calculated the real part of the self-energy within the BCS theory and his results show a maximum downward shift at $\hbar\omega = 2\Delta$ in qualitative agreement with the observations of Fig. 13. Early ultrasonic experiments,¹⁴ working in a much lower frequency regime have also shown a decrease in the velocity of sound on entering the superconducting phase. The effect is much smaller than observed in the present experiment but was observed in Pb, V, Ta, and Nb. Recent inelastic neutron scattering experiments³¹ on Nb_3Sn have also shown a small decrease in phonon frequency on cooling into the superconducting phase. It thus appears that when a metal becomes superconducting, there is a renormalization to lower frequencies of the small- q acoustic phonons.

Even less well understood, and perhaps more fundamental, is the more drastic softening of the

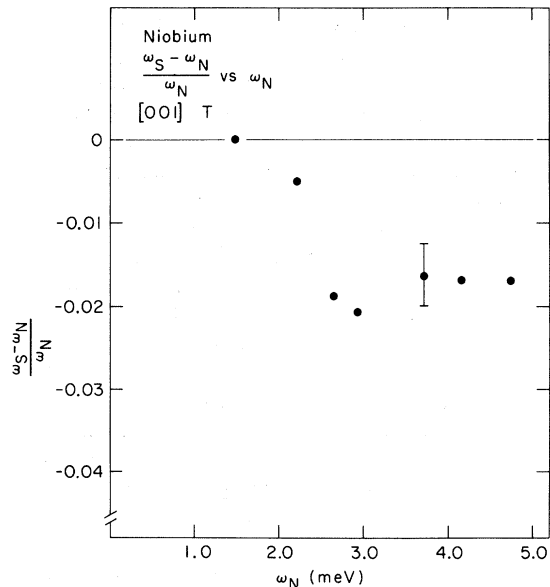


FIG. 13. Fractional change of the frequency of the $[001]T$ phonons as a function of energy. ω_N is taken as the value of the frequency at $T=10^\circ\text{K}$ and ω_S is the value near 1.2°K . Minimum corresponds closely to the value of $2\Delta(0)$.

[00 ξ]T branch that occurs for $T > T_c$. The strange q dependence of this branch for $\xi > 0.1$ also is not well understood. Unusual phonon dispersion has been observed in several other transition metal³²⁻³⁴ and some transition-metal carbides.³⁵ The correlation exists that the more unusual the dispersion curve the higher the T_c .³⁵ Recently Weber *et al.*³⁶ and Weber³⁷ have explained the anomalies in the longitudinal branches of the transition-metal carbides and succeeded in predicting an anomaly in the transverse-acoustic branches which has since been observed.³⁸ The anomalies Weber *et al.* have treated, however, are localized in a small region in q space. There is no theory as yet to explain the anomaly in the [001]T branch, which is extended over most of the zone. It is undoubtedly related to some form of electron-phonon interaction. Chui has been able to explain the dip in the [001]L branch of Nb and its absence in Mo, but he did not explain the behavior of the transverse branches.³⁹ A more complete understanding of the electron-phonon interactions at temperatures

well above T_c and its relation to superconductivity is needed.

V. CONCLUSION

In conclusion, we have confirmed via inelastic neutron scattering several features of the BCS theory of high-frequency sound attenuation in superconductors. The attenuation is composed of two parts: (i) the smoothly temperature-dependent behavior due to interaction of the phonon with thermally excited quasiparticles, and (ii) a pair breaking at $\hbar\omega_p \geq 2\Delta(T)$ which is due to the energetically favorable breakup of Cooper pairs by the phonon. A discontinuity occurs at $\hbar\omega_p = 2\Delta(T)$ and agrees well with the calculation.

ACKNOWLEDGMENTS

We thank P. B. Allen and H. G. Schuster for the many informative and stimulating discussions and, in particular, P. B. Allen for the critical reading of the manuscript.

*Work performed under the auspices of the U.S. Energy Research and Development Administration.

¹For a comprehensive review of superconductivity, see J. R. Schrieffer, *Theory of Superconductivity* (Benjamin, New York, 1964).

²J. Bardeen, L. N. Cooper, and J. R. Schrieffer, *Phys. Rev.* **106**, 162 (1957), referred to as BCS.

³W. L. McMillan, *Phys. Rev.* **167**, 331 (1968).

⁴W. L. McMillan and J. M. Rowell, in *Superconductivity*, edited by R. D. Parks (Dekker, New York, 1969).

⁵P. B. Allen, *Phys. Rev. B* **6**, 2577 (1972); *Solid State Commun.* **14**, 937 (1974).

⁶J. A. Reissland, *The Physics of Phonons* (Wiley, New York, 1973), pp. 225 ff.

⁷See G. Gladstone, M. A. Jensen, and J. R. Schrieffer, in *Superconductivity*, edited by R. D. Parks (Dekker, New York, 1969).

⁸A. Privorotskii, *Zh. Eksp. Teor. Fiz.* **43**, 1331 (1962) [*Sov. Phys. -JETP* **16**, 945 (1963)].

⁹V. M. Bobetic, *Phys. Rev.* **136**, A1535 (1964).

¹⁰J. A. Snow, *Phys. Rev.* **172**, 455 (1968).

¹¹T. A. Fagan and M. P. Garfunkel, *Phys. Rev. Lett.* **18**, 897 (1967); E. R. Dobbs, E. Hughes, M. J. Lea, J. A. Rayne, and C. K. Jones, in *Proceedings of the Twelfth International Conference on Low Temperature Physics—Kyoto*, edited by E. Kaude (Academic Press of Japan, Kyoto, 1971), p. 277.

¹²J. D. Axe and G. Shirane, *Phys. Rev. Lett.* **30**, 214 (1973); *Phys. Rev. B* **8**, 1965 (1973).

¹³G. Shirane, J. D. Axe, and S. M. Shapiro, *Solid State Commun.* **13**, 1893 (1973).

¹⁴G. A. Alers and D. L. Naldorf, *Phys. Rev. Lett.* **6**, 677 (1961).

¹⁵See R. A. Cowley, in *Phonons in Perfect Lattice and in Lattices with Point Defects*, edited by R. W. Stevensen (Wiley, New York, 1966).

¹⁶H. G. Schuster, *Solid State Commun.* **13**, 1559 (1973).

¹⁷Material Research Corp., Orangeburg, N. Y. 10962.

¹⁸M. J. Cooper and R. Nathans, *Acta Cryst.* **23**, 357 (1967).

¹⁹S. A. Werner and R. Pynn, *J. Appl. Phys.* **42**, 4736 (1971); R. Pynn and S. A. Werner, laboratory report AE-FF-112, A. B. Atomenergi, Studsvik, Sweden (unpublished).

²⁰D. W. Poesner, *Aust. J. Phys.* **12**, 184 (1959); G. K. Wertheim, M. A. Butler, K. W. West, and D. N. E. Buchanan, *Rev. Sci. Instrum.* **45**, 1369 (1974).

²¹J. Bostock, K. Agyeman, M. H. Frommer, and M. L. A. MacVicar, *J. Appl. Phys.* **44**, 6567 (1973).

²²D. K. Finnemore, T. F. Stromberg, and C. A. Swenson, *Phys. Rev.* **149**, 231 (1966).

²³See P. G. De Gennes, *Superconductivity of Metals and Alloys* (Benjamin, New York, 1966); J. R. Liebowitz and K. Fossheim, *Phys. Rev. Lett.* **21**, 1246 (1968).

²⁴Y. Nakagawa and A. D. B. Woods, in *Proceedings of International Conference on Lattice Dynamics*, edited by R. F. Wallis (Pergamon, New York, 1963), p. 39.

²⁵B. M. Powell, A. D. B. Woods, and P. Martell, in *Neutron Inelastic Scattering 1972* (International Atomic Energy Agency, Vienna, 1972), p. 43.

²⁶B. M. Powell, P. Martell, and A. D. B. Woods, *Phys. Rev.* **171**, 727 (1968).

²⁷K. Fossheim, *Phys. Rev. Lett.* **19**, 81 (1967).

²⁸The parameters used in the calculations are taken from Ref. 5 and P. B. Allen (private communication). $N_c(0) = 0.91$ states/eV atom, $\lambda = 0.83$, $\langle\omega\rangle = 15.8$ meV.

²⁹P. B. Allen, International Conference, Physics in High Magnetic Fields, Grenoble, 1974 (unpublished).

³⁰P. B. Allen, *Solid State Commun.* **3**, 311 (1973).

³¹See Ref. 12, Fig. 1 of *Phys. Rev. Lett.* **30**, 214 (1973).

³²R. Collella and B. W. Batterman, *Phys. Rev. B* **1**, 3413 (1970).

³³A. D. B. Woods, *Phys. Rev.* **136**, A781 (1964).

³⁴A. D. B. Woods and S. H. Chen, *Solid State Commun.* **2**, 233 (1964).

³⁵H. G. Smith, *AIP Conf. Proc.* **4**, 321 (1972).

³⁶W. Weber, H. Bilz and U. Schröder, Phys. Rev. Lett. 28, 600 (1972).

³⁷W. Weber, Phys. Rev. B 8, 5082 (1973); 8, 5093

(1973).

³⁸H. G. Smith, Phys. Rev. Lett. 29, 353 (1972).

³⁹S. T. Chui, Phys. Rev. B 9, 3300 (1974).